Proceedings of the Seventh Annual ASME Verification and Validation Symposium
ASME2018-V&VS
May 16 - 18, 2018, Minneapolis, MN

VVS2018-9320

FINITE ELEMENT METHOD SOLUTION UNCERTAINTY, ASYMPTOTIC SOLUTION, AND A NEW APPROACH TO ACCURACY ASSESSMENT

Jeffrey T. Fong
National Institute of Standards & Technology
Gaithersburg MD 20899 U.S.A.
fong@nist.gov

Pedro V. Marcal
MPACT Corp.
Oak Park CA 91377 U.S.A.
pedrovmarcal@gmail.com

Robert Rainsberger
XYZ Scientific Applications, Inc.
Pleasant Hill, CA 95425 U.S.A.
r.rainsberger@yahoo.com

Li Ma
Theiss Research
La Jolla, CA 92037 U.S.A.
li.ma@nist.gov lilyma01@yahoo.com

N. Alan Heckert, and James J, Filliben
National Institute of Standards & Technology
Gaithersburg MD 20899 U.S.A.
alan.heckert@nist.gov filliben@nist.gov

ABSTRACT

Errors and uncertainties in finite element method (FEM) computing can come from the following eight sources, the first four being FEM-method-specific, and the second four, model-specific: (1) Computing platform such as ABAQUS, ANSYS, COMSOL, LS-DYNA, etc.; (2) choice of element types in designing a mesh; (3) choice of mean element density or degrees of freedom (d.o.f.) in the same mesh design; (4) choice of a percent relative error (PRE) or the Rate of PRE per d.o.f. on a log-log plot to assure solution convergence; (5) uncertainty in geometric parameters of the model; (6) uncertainty in physical and material property parameters of the model; (7) uncertainty in loading parameters of the model, and (8) uncertainty in the choice of the model. By considering every FEM solution as the result of a numerical experiment for a fixed model, a purely mathematical problem, i.e., solution verification, can be addressed by first quantifying the errors and uncertainties due to the first four of the eight sources listed above, and then developing numerical algorithms and easy-to-use metrics to assess the solution accuracy of all candidate solutions. In this paper, we present a new approach to FEM verification by applying three mathematical methods and formulating three metrics for solution accuracy assessment. The three methods are: (1) A 4-parameter logistic function to find an asymptotic solution of FEM simulations; (2) the nonlinear least squares method in combination with the logistic function to find an estimate of the 95 % confidence bounds of the asymptotic solution; and (3) the definition of the Jacobian of a single finite element in order to compute the Jacobians of all elements in a FEM mesh. Using those three methods, we develop numerical tools to estimate (a) the uncertainty of a FEM solution at one billion d.o.f., (b) the gain in the rate of PRE per d.o.f. as the asymptotic solution approaches very large d.o.f.'s, and (c) the estimated mean of the Jacobian distribution (mJ) of a given mesh design. Those three quantities are shown to be useful metrics to assess the accuracy of candidate solutions in order to arrive at a so-called "best" estimate with uncertainty quantification. Our results include calibration of those three metrics using problems of known analytical

solutions and the application of the metrics to sample problems, of which no theoretical solution is known to exist.

Keywords: ABAQUS; Accuracy assessment metric (AAM); ANSYS; barrel vault; cantilever beam; computational modeling; COMSOL; DATAPLOT; element type; FEM; finite element method; hexahedron element; holed composite laminate strength test; Jacobian; logistic function; LS-DYNA; mesh density; mesh quality; MPACT; nonlinear least squares method; relative error convergence rate; resonance frequency; statistical analysis; super-parametric method; tetrahedron element; TrueGrid; uncertainty quantification.

1. INTRODUCTION

Since 1991, five international conferences on numerical simulation of 3-D sheet forming processes (NUMISHEET) have taken place at two- or three-year intervals (Switzerland, 1991, Japan, 1993, United States, 1996, France, 1999, and Korea, 2002).

The concept of "virtual manufacturing" had taken hold among participants of those conferences, as noted by the editors of the proceedings of the 2002 conference in its foreword [1] that "the numerical method plays a key role in simulation of sheet metal forming processes for design innovation through virtual manufacturing."

Since metrology had always played a key role in traditional manufacturing, a need for "virtual metrology" arose in the then new field of "virtual manufacturing." After the 1996 NUMISHEET Conference held in the United States, a benchmark committee was formed to launch an inter-laboratory experimental and numerical simulation project costing around $9 Million with the U.S. National Institute of Standards and Technology (NIST) contributing $4.3 Million through its Advanced Technology Program. Results of that project was presented at the 2002 NUMISHEET Conference held in Korea [1] . Three benchmark test problems were selected with two materials specified for the first two test problems and one material for the third. Details of the project are shown below:

Test	Problem	Experimental	Simulation
A.	Deep drawing of a cylindrical cup.	7 teams	14 teams
B.	**Unconstrained cylindrical bending.**	**4 teams**	**17 teams**
C.	Forming of a front bender.	1 team	10 teams

Of the three benchmark test problems, Test B had the largest number of participating teams in simulation, so we choose a specific case of Test B (1.0-mm thick 6111-T4 aluminum sheets) for presentation in this paper as an example to motivate a need to develop finite element analysis (FEA) accuracy assessment metrics (AAMs).

In Figs. 1 and 2, we show a graphical representation of the test problem together with a list of 4 experimental teams, BE-1 through BE-4, and 17 simulation teams, BS-1 through BS-17. In Fig. 3, we show a graphical comparison of the simulation results of 15 teams vs. the experimental result of one team (BE-1), with the computational environment data for each simulation team listed in Fig. 4.

A closer look at Figs. 3 and 4 led us to conclude that the NUMISHEET/NIST project was inadequately conceived by asking each team to make only one FEA run with different mesh design and computational environment such that it was impossible to conduct a proper inter-laboratory comparison analysis, nor an uncertainty analysis in the absence of a statistical design of experiments. No requirement was specified for each team to conduct a verification study of the simulation result, a step that has now received attention in the literature (see, e.g., [2] - [7]). In short, the project failed to contribute significant advances to the accuracy assessment of FEA.

It is well known (see, e.g., Ref. [2]) that errors and uncertainties in FEA computing can come from the following eight sources, the first four being FEA-method-specific, and the second four, model-specific: (1) Computing platform such as ABAQUS, ANSYS, COMSOL, LS-DYNA, MPACT [8-12], etc.; (2) choice of element types in designing a mesh; (3) choice of mean element density or degrees of freedom (d.o.f.) in the same mesh design; (4) choice of a percent relative error (PRE) or the Rate of PRE per d.o.f. on a log-log plot to assure solution convergence; (5) uncertainty in geometric parameters of the model; (6) uncertainty in physical and material property parameters of the model; (7) uncertainty in loading parameters of the model, and (8) uncertainty in the choice of the model. By considering every FEM solution as the result of a numerical experiment for a fixed model, a purely mathematical problem, i.e., solution verification, can be addressed by first quantifying the errors and uncertainties due to the first four of the eight sources listed above, and then developing numerical algorithms and metrics to assess the solution accuracy of all candidate solutions.

In Sections 2 and 3, we present a method to obtain the asymptotic solution using a sequence of FEA candidate solutions, as well as an estimate of the solution uncertainty as AAM-1. In Sections 4 and 5, we formulate two more metrics, AAM-2 and AAM-3. In Section 6, we calibrate the usefulness of all three metrics using four problems of known exact solutions. In Sections 7 and 8, we present application to two problems, of which no solutions are known to exist. A discussion of the significance of our method, metrics, and results appear in Section 9, and some concluding remarks in Section 10. A lsit of referneces is given in Section 11.

2. A NONLINEAR LEAST SQUARES LOGISTIC FIT

A logistic function [13], named after Pierre Francois Verhulst [14] for his use in a study of population growth, is a flat-S curve with two horizontal asymptotes. It is commonly represented by the following 4-parameter equation:

$$f(x) = y_1 - L^*\{ \exp(-k^*(x-a)) / (1+\exp(-k^*(x-a))) \}, \qquad (1)$$

where y_1 is the upper right asymptote with x approaching infinity, $L = y_1 - y_0$ with y_0 equal to the lower left asymptote with x going left to the negative infinity, k is the flat-S shape steepness coefficient, and a , the x-value of the flat-S curve midpoint (sometimes denoted by x_0).

To visualize this 4-parameter function, let us simplify it by assigning $y_0 = 0$, and $y_1 = 1$. Eq. (1) thus becomes a 2-parameter logistic function with two sample plots given in Fig. 5. The parameter L is, therefore, a scale factor for the difference between the lower and the upper asymptotes.

Given a sequence of N ($N_{min} = 5$) FEA candidate single-valued solutions of increasing mesh density, or, degrees of freedom (d.o.f.), and assuming that the candidates are monotonically increasing, we can use a 4-parameter logistic function, given by Eq. (1), to conduct a nonlinear least squares fit of the N data [15, 16] and obtain an asymptotic solution, y_1 , at very large d.o.f. with a 95 % confidence band.

In Fig. 6, we show an example of finding the maximum Mises stress in a wrench using 10 candidate solutions of FEA COMSOL runs [10] and a nonlinear least squares logistic function fit [17].

It is interesting to note that when we used the coarsest mesh, the candidate solution was about 320 MPa. As we increased the mesh density or d.o.f., the stress rose monotonically. When we completed a 17-candidate FEA run with d.o.f. reaching 6 million, the solution levelled off to 369.72 MPa, about 15 % higher than the initial candidate. When we applied the nonlinear least squares logistic function fit with $N = 10$, the asymptotic solution was 369.1 MPa, which differed from 369.72 by only 0.2 %. More interestingly, the fit yielded an estimate of uncertainty at a billion d.o.f with 95 % confidence equal to 1.92 %, which is a new result of tremendous importance to FEA accuracy assessment.

For decreasing candidate FEA solutions, Eq. (1) becomes

$$f(x) = y_1 + L^*\{ \exp(-k^*(x-a)) / (1+\exp(-k^*(x-a))) \}, \qquad (2)$$

In some FEA problems, we deal with quantities that are known to be either zero or positive-definite (e.g., a Mises stress). Eqs. (1) and (2) can be further simplified with $y_0 = 0$ and $y_1 = L$. Thus, Eq. (1) becomes a 3-parameter function as follows:

$$f(x) = y_1 / (1 + \exp(-k * (x-a))). \qquad (3)$$

3. ACCURACY ASSESSMENT METRIC (AAM) NO. 1

The nonlinear logistic model of the N ($N > 4$) candidate solutions of a specific FEA computational code with increasing mesh density (or, d.o.f.) produces not only an asymptotic solution at infinite d.o.f., but also a 95 % confidence band, with which one can estimate a quantity to be called the "FEA Solution Uncertainty," or, simply, "Uncertainty" at an arbitrarily large d.o.f.

In Figs. 7 and 8, we illustrate this Uncertainty concept with an example that we published in a 2008 paper [7] for estimating the first resonance bending frequency of a cantilever beam in an atomic force microscope. The beam dimensions were 232 μm long, 34 μm wide, and 7 μm thick. The material is assumed to be isotropic (polycrystal silicon) and elastic with a Young's modulus of 169,158 MPa, and density of 2.329 E-9 ton/cu. mm. Based on the classical theory of elastic simple beams [18, p.338], the first resonance frequency for bending is 179.03 kHz.

In Fig. 7, we show that a 5-candidate-ABAQUS-Hex-08-solution fit yielded an asymptotic solution equal to 180.69 kHz, which differs from the exact solution by 0.93 %. In Fig. 8, which is an enlarged view of the asymptotic solution near infinite d.o.f., we show the 95 % confidence band with a specific upper and lower bound at one billion d.o.f. equal to 180.72 and 180.66 kHz, respectively.

For the purpose of this paper, we define "Uncertainty" to be the difference between the upper bound and the asymptotic solution at one billion d.o.f., which in our example happened to be 180.72 - 180.69 = 0.03 kHz. Using our fit algorithm, we can deliver an asymptotic solution with uncertainty in the form of 180.69 +/- 0.03 kHz , which unfortunately is still off the mark as compared with the exact solution. Nevertheless, this definition provides a plausible candidate as a metric for FEA accuracy assessment, and we shall find out in Section 6 whether it is a useful metric to be known as AAM-1, or simply, M-1.

4. ACCURACY ASSESSMENT METRIC (AAM) NO. 2

In Fig. 9, we illustrate a definition of a second metric to be known as AAM-2, or simply, M-2, by returning to the problem of fitting 10 candidate COMSOL solutions of finding the maximum Mises stress in a wrench as shown in Fig. 6. We are now interested in the convergence behavior (in blue color) of the 10 candidate solutions at about 100,000 d.o.f. versus that of the asymptotic solution (in red) near 100 million d.o.f.

Let $u_1(xx_1)$, $u_2(xx_2)$, $u_3(xx_3)$, $u_4(xx_4)$, $u_5(xx_5)$ be the five candidate FEA solutions of increasing d.o.f.'s, X_1, X_2, X_3, X_4, X_5, with $xx_1 = Log_{10} X_1$, $xx_2 = Log_{10} X_2$, $xx_3 = Log_{10} X_3$, $xx_4 = Log_{10} X_4$, $xx_5 = Log_{10} X_5$. For i = 2, 3, 4, 5, we define the i-th "Percent Relative Error," or, PRE_i , as follows:

$$PRE_i(xx_i) = abs\{ 100 * [u_i(xx_i) - u_{i-1}] / u_{i-1} \} \qquad (4)$$

Let $LPRE_i = Log_{10}(PRE_i)$, *plot* $LPRE_i$ *vs.* xx_i on a log-log paper, as shown in Fig. 9 in blue color, and use a linear least squares fit to obtrain a straight line with a slope, c_0 , that represents the convergence behavior of the 5 candidate solution

We now need the model-predicted asymptotic solution to deliver a similar slope, c_1, representing the convergence behavior of the model near 100 million d.o.f. using a definition for a series of PRE_i identical to that of Eq. (4). Ideally, c_1 should be close to zero. Let us now define a metric equal to the difference between c_1 and c_0, and call it a "Gain," $g = c_1 - c_0$, with g defined as the metric AAM-2, or simply, M-2.

5. ACCURACY ASSESSMENT METRIC (AAM) NO. 3

Both AAM-1 and AAM-2 are *a posteriori* metrics in the sense that they are estimated after a computer simulation such as an FEA run is completed. Given a finite element mesh design, with a fixed choice of mesh density, element type(s), and geometric configuration, it is tempting to ask if an *a apriori* metric exists first to assess the mesh "quality" and then, perhaps, the accuracy of a subsequent FEA run.

The answer lies in a close examination of a classical FEA concept known as the determinant of the Jacobian matrix, or simply, the Jacobian [2]. Using a FEA pre-processor named *TrueGrid* [19], Rainsberger, Fong and Marcal wrote a paper [20], in which a metric, AAM-3, or simply, M-3, was defined as a pair of numbers representing the mean, mJ, and standard deviation, sdJ, of a distribution of Jacobian's at every node in a finite element mesh.

For this paper, we will only sketch the concept of a Jacobian without defining the metric, AAM-3. Each element is defined by a set of ordered nodes with coordinates $p_i = (x_i, y_i, z_i)$ for i between 1 and m, where m is the number of nodes in the element. Associated with each node is a scalar shape function, $N_i (\xi, \eta, \zeta)$. For each node, p_i , we define the Jacobian matrix, $\mathbf{J}$, as follows:

$$\begin{Bmatrix} \dfrac{\partial N_i}{\partial \xi} \\ \dfrac{\partial N_i}{\partial \eta} \\ \dfrac{\partial N_i}{\partial \zeta} \end{Bmatrix} = \begin{bmatrix} \dfrac{\partial x}{\partial \xi}, & \dfrac{\partial y}{\partial \xi}, & \dfrac{\partial z}{\partial \xi} \\ \dfrac{\partial x}{\partial \eta}, & \dfrac{\partial y}{\partial \eta}, & \dfrac{\partial z}{\partial \eta} \\ \dfrac{\partial x}{\partial \zeta}, & \dfrac{\partial y}{\partial \zeta}, & \dfrac{\partial z}{\partial \zeta} \end{bmatrix} \begin{Bmatrix} \dfrac{\partial N_i}{\partial x} \\ \dfrac{\partial N_i}{\partial y} \\ \dfrac{\partial N_i}{\partial z} \end{Bmatrix} = \mathbf{J} \begin{Bmatrix} \dfrac{\partial N_i}{\partial x} \\ \dfrac{\partial N_i}{\partial y} \\ \dfrac{\partial N_i}{\partial z} \end{Bmatrix}. \tag{5}$$

The determinant of the matrix, $\mathbf{J}$, is called the Jacobian, J , which needs to be evaluated at every node of a finite element mesh. The set of all such Jacobian's forms a distribution with its mean value, mJ , and standard deviation, sdJ , which can be estimated for any finite element mesh using a macro written in *TrueGrid* [19]. For this paper, we will define the third metric, AAM-3, or simply, M-3, as the quantity, mJ .

In Fig. 10, we illustrate the use of a TrueGrid [19] macro to find the distribution of Jacobian's in a specific mesh design. A graphical display of the distribution of the Jacobian's is given in the right of the figure, with the mean of the Jacobian, mJ , given in the top box as 4.011077E+00.

6. FOUR BENCHMARKS FOR CALIBATING AAM'S

We are now ready to calibrate the three metrics, AAM-1, -2, and -3, using four FEA benchmark problems, each of which has a known exact solution. In Fig. 11, we show the FEA (ABAQUS) solutions of a resonance frequency problem [18] with six mesh designs of different mean aspect ratios (MAR). All three metrics correlate exceedingly well with the solution accuracy of the six meshes using a single platform.

In Fig. 12, we show the FEA (COMSOL) solutions of a wrench max. Mises stress problem [10, 17] with four teams of 6, 7, 8, and 9 candidate solutions. Again AAM-1 and -2 correlate exceedingly well. We expect AAM-3 to pass the test as well even though no computation was done for lack of time.

For a single platform, we observe that AAM-1 (uncertainty) performs well because the complication due to platform was absent. AAM-1 (uncertainty) is not expected to work as an accuracy assessment metric when it comes to a multi-platform competition. In Fig. 13, we return to the resonance frequency problem using four platforms, namely ABAQUS, COMSOL, LSDYNA, and MPACT, and obtain an interesting result that only AAM-2 (Gain in slope of Log_{10}(PRE) vs. Log_{10}(d.o.f.) plot) works as a viable accuracy assessment metric.

In Fig. 14, we confirmed the above new result that only AAM-2 works for a multi-platform competition by introducing the classical cantilever max. stress problem with two FEA platforms, ABAQUS and MPACT.

7. APPLICATION EXAMPLE FOR SINGLE PLATFORM

We now apply the new FEA accuracy assessment methodology to problems of which no exact solution exists. Our first example is for a single platform (ABAQUS) 2D FEA problem for a holed composite laminate strength test. In Fig. 15, we show that both AAM-1 and -2 work well in being able to pick a winner without hesitation [21].

8. APPLICATION EXAMPLE FOR MULTI-PLATFORM

Our next application is to work on a classical barrel vault max. displacement problem using two platforms, namely ABAQUS and MPACT. As shown in Fig. 16, the AAM-2 (Gain in slope) works quite well, and the AAM-1 (uncertainty) performs rather weakly. It is, however, encouraging that AAM-2 works in all cases tested so far.

9. DISCUSSION

The introduction of a new method for finding an asymptotic FEA solution with confidence bounds and uncertainty quantification is innovative in advancing the state of the art and science of computational modeling. The subsequent formulation, calibration, and testing of three FEA accuracy assessment metrics is significant in adding a new tool to the toolbox of FEA verification.

10. CONCLUDING REMARKS

Finite element method (FEM) and the mathematics of the verification and validation (V & V) of its computational results have been of interest to engineers and scientists since the 1960s. Difficulties in modeling "correctly" and computing "accurately" for large-scale practical problems involving complex geometry and uncertainty in governing equations and physical parameters have created a need to develop efficient methods and subsequently recommended practices of FEM V & V. The availability of many commercial FEM codes that are increasingly user-friendly has complicated the problem of answering the fundamental question, "is the FEM result correct, and what are its confidence bounds?" By considering every FEM solution as the result of a numerical experiment and by using a combination of three mathematical and computational methods, we have developed in this paper a new approach to the V & V of FEM.

11. REFERENCES

[1] Yang, D., Oh, S. L., Huh, H., and Kim, Y. H., eds., "Numisheet 2002: Design Innovation Through Virtual Manufacturing," *Proc. 5th Int. Conf. and Workshop on Numerical Simulation of 3D Sheet Forming Processes - Verification of Simulation and Experiment*, 21-25 October 2002, Jeju Island, Korea, Vol. 2, published by Korea Advanced Inst. of Science and Technology (KAIST), 373-1, Science Town, Taejon, 305-701, Korea, 2002.

[2] Zienkiewicz, O. C., and Taylor, R. L., 2000, *The Finite Element Method, Volume 1: The Basis*, 5th ed. Butterworth-Heinemann (2000).

[3] Oberkampf, W. L., and Roy, C. J., 2010, Verification and Validation in Scientific Computing. Cambridge University Press, 2010.

[4] Barone, M. F., Oberkampf, W. L., and Blottner, F. G., 2006, "Validation case study: prediction of compressible turbulent mixing layer growth rate," *AIAA Journal*, **44**(7), pp. 1488-1497, 2006.

[5] Oberkampf, W. L., and Barone, M. F., 2006, "Measures of agreement between computation and experiment: Validation metrics," *J. Comput. Phys*., **217**, pp. 5-36, 2006.

[6] Box, G. E. P., Hunter, W. G., and Hunter, J. S., 1978, *Statistics for Experimenters*, 1st ed. Wiley, 1978.

[7] Fong, J. T., Filliben, J. J., Heckert, N. A., and deWit, R., 2008, "Design of Experiments Approach to Verification and Uncertainty Estimation of Simulations based on Finite Element Method," in *Proc. Conf. Amer. Soc. for Eng. Education*, June 22-25, 2008, Pittsburgh, PA, Paper No. AC2008-2725, 2008.

[8] Anon., 2015, Abaqus/CAE User's Guide, and Abaqus Analysis User's Guide, version 6.13. Dassault Systemes Simulia Corp., Providence, RI, U.S.A.,http://www.3ds.com/products-services/simulia/support/documentation/, 2015.

[9] Anon., 2015, Ansys Multiphysics User's Manual, Release 16.0. ANSYS, Inc., Canonsburg, PA, U.S.A., http://www.ansys.com/Support/Documentation, 2015.

[10] Anon., 2015, Introduction to COMSOL Multiphysics, version 5.1. Burlington, MA: COMSOL, Inc., http://cdn.comsol.com/documentation/5.1.0.180/IntroductionToCOMSOLMultiphysics.pdf, 2015.

[11] Anon., 2015, LS-DYNA R8.0 Keyword Manual Vols. I, II, and III. Livermore Software Technology Corp., 7374 Las Positas Road, Livermore, CA 94551, U.S.A., http://www.lstc.com/, 2015.

[12] Marcal, P. V., 2001, MPACT User Manual. Published by Mpact Corp., Oak Park, CA 91377, pedrovmarcal@gmail.com, 2001.

[13] Evans, M., Hastings, N., and Peacock, B., 2000, Statistical Distributions, 3rd ed., pp. 124-128. Wiley, 2000.

[14] Verhulst, P. F., 1845, "Recherches mathematiques sur la loi d'accroissement de la population," [Mathematical Rese arches into the Law of Population Growth Increase], re-published in *Nouveaux Memoires de l'Academie Royaledes Sciences et Belles-Lettres de Bruxelles*, **18**, pp. 1-42, 2013.

[15] Draper, N. R., and Smith, H., 1966, Applied Regression Analysis, Chapters 1-3, pp. 1-103, and Chapter 10, pp. 263-304. Wiley, 1966.

[16] Filliben, J. J., and Heckert, N. A., 2002, Dataplot: A Statistical Data Analysis Software System, National Institute of Standards & Technology, Gaithersburg, MD 20899, http://www.itl.nist.gov/div898/software/dataplot.html, 2002.

[17] Fong, J. T., Heckert, N. A., Filliben, J. J., Marcal, P. V., Rainsberger, R., and Ma, L., 2015, "Uncertainty Quantification of Stresses in a Cracked Pipe Elbow Weldment Using a Logistic Function Fit, a Nonlinear Least Squares Algorithm, and a Super-parametric Method," *Procedia Engineering*, **130** (2015), 135-149, available online at www.sciencedirect.com, 2015.

[18] Timoshenko, S., and Young, D. H., 1955, Vibration Problems in Engineering, 3rd ed. D. Van Nostrand, 1955.

[19] Rainsberger, R., 2014, TrueGrid User's Manual: A Guide and a Reference, Volumes I, II, and III, Version 3.0.0. Published by XYZ Scientific Applications, Inc., Pleasant Hill, CA 94523, www.truegrid.com/pub/TGMAN300.1.pdf, 2014.

[20] Rainsberger, R., Fong, J. T., and Marcal, P. V., 2018, "Application of an *a priori* Jacobian-based Error Estimation Metric to the Accuracy Assessment of 3D FEM Simulation," to appear in Proc. ASME PVP Conference, July 20-25, 2018, Prague, the Czech Republic, Paper No. PVP2018-84784, *http://www.asmeconferences.org/pvp2018*, 2018.

[21] Ma, L., Fong, J. T., Heckert, N. A., and Filliben, J. J., 2018, "Uncertainty Quantification of Finite Element Analysis of Uni-axial Strength Test Holed Composite Laminates," to appear in Proc. ASME PVP Conference, July 20-25, 2018, Prague, the Czech Republic, Paper No. PVP2018-84730, *http://www.asmeconferences.org/pvp2018*, 2018.

Benchmark Test B

Unconstrained Cylindrical Bending

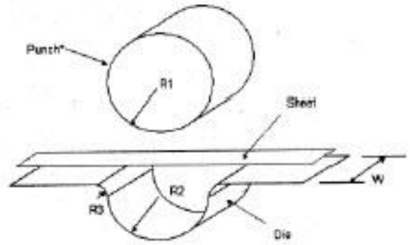

R1=23.5, R2=25.0, R3=4, W=50 (Unit : mm)
Figure B.1 Tool for Unconstrained Cylindrical Bending

PARTICIPANTS FOR BENCHMARK B

Number	Name	Affiliation	Country
	EXPERIMENTS		
BE-01	Hyung-Jong Kim	Kangwon National Univ.	Korea
BE-02	Pierre-Yves Manach, Guillaume Gúerin and Sandrine Thuillier	Cedex	France
BE-03	Margot Klaassen and Eisso Atzema	Corus Research	The Netherlands
BE-04	Xiao-Xing Li, Dong-Sheng Li, and Xian-Bin Zhou	Beijing Univ. of Aeronautics and Astronautics	P. R. China

Fig. 1. List of 4 teams, BE-01, through BE-04, who agreed to participate in an Inter-Laboratory Experimental Benchmark Test (Numisheet/NIST 2002) for the unconstraind cylindrical bending of 1.0-mm-thick sheets of aluminum and high-strength steel.

Benchmark Test B

Unconstrained Cylindrical Bending

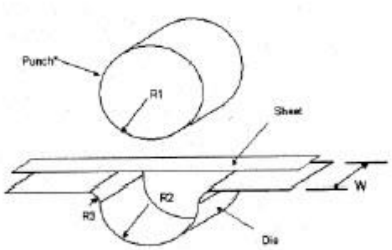

R1=23.5, R2=25.0, R3=4, W=50 (Unit : mm)
Figure B.1 Tool for Unconstrained Cylindrical Bending

	SIMULATIONS		
BS-01	Eugenio Oñate Ibañez De Navarra, Alberto Ferriz, and Oscar Fruitós CIMNE	CIMNE	Spain
BS-02	Ming Chen	United States Steel Corp.	USA
BS-03	Tony Chang and Wei Wang	Rouge Steel Co.	USA
BS-04	Francis Sabourin	INSA - Lyon	France
BS-05	Satoshi Ikeda	ESTECH Corp.	Japan
BS-06	Margot Klaassen and Eisso Atzema	Corus Research	The Netherlands
BS-07	Siguang Xu, Ramesh Joshi, and Chuan-Tao Wang	General Motors Corp.	USA
BS-08	Jun Park	Hibbitt, Karlsson & Sorensen, Inc.	USA
BS-09	Bin Zhang, Dongsheng Li, and Xianbin Zhou	Beijing Univ. of Aeronautics and Astronautics	P. R. China
BS-10	M. C. Oliveira, J. L. Alves, and L. F. Menezes	Univ. of Coimbra	Portugal
BS-11	Chung-Souk Han and Robert H. Wagoner	The Ohio State Univ.	USA
BS-12	Margot Klaassen and Eisso Atzema	Corus Research	The Netherlands
BS-13	Seung-Geun Lee, Yangwook Choi, and J. K. Lee	The Ohio State Univ.	USA
BS-14	Maki Nagakura, Masato Takamura, and Ohura Kenichi	The Institute of Physical & Chemical Research	Japan
BS-15	Margot Klaassen and Eisso Atzema	Corus Research	The Netherlands
BS-16	Siguang Xu, Ramesh Joshi, and Chuan-Tao Wang	General Motors Corp.	USA
BS-17	Yongming Kong, Wan Cheng, and Decai Jia	Altair Engineering Ltd.	P. R. China

Fig. 2. List of 17 teams, BS-01 through BS-17, who agreed to participate in an Inter-Laboratory Numerical Simulation Benchmark Exercise (Numisheet/NIST 2002) for the unconstrained cylindrical bending of 1.0-mm-thick Al & Steel Sheets.

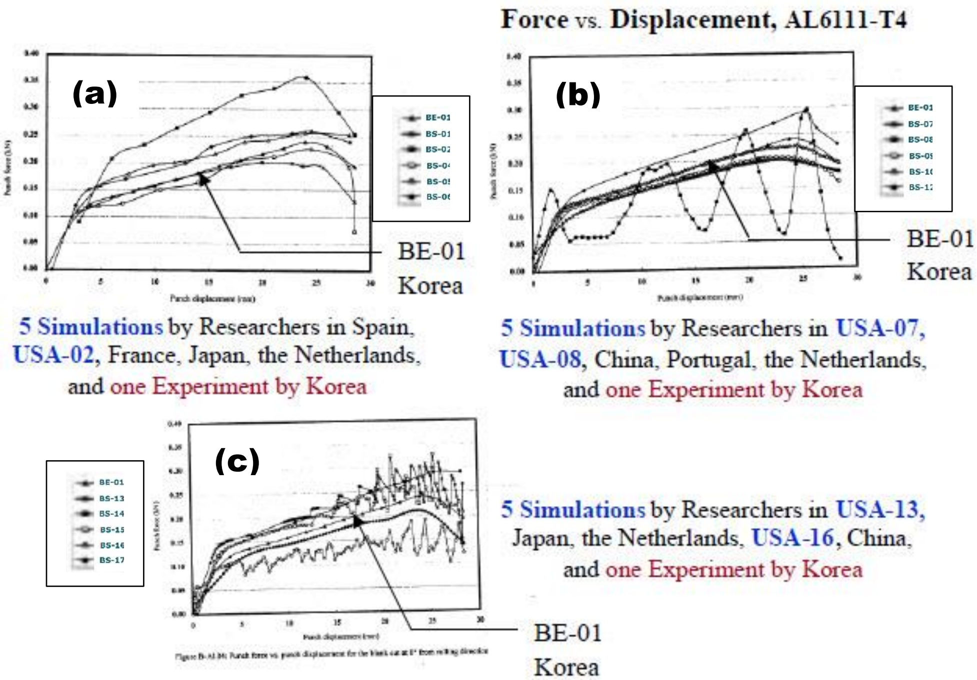

Fig. 3. Simulated force vs. displacement results of (a) Teams BS-01, -02, -04, -05, -06, (b) Teams BS-07, -08, -09, -10, -12, and (c) Teams BS-13 through BS-17, vs. that of a typical experimental team (BE-01, Korea) for the benchmark test problem.

Team ID	FEA Formulation	FEA Code	No. of Elem.	CPU (Min.)	Computer Name	Team Company	Team Country
BS-01	Explicit-implicit	STAMPACK	7,500	1,600	Pentium III	CIMNE	Spain
BS-02	Explicit-implicit	LS-DYNA3D	1,500	3,000	SGI Origin 2000	U.S. Steel	USA
BS-03	Explicit-implicit	LS-DYNA3D	594	135	COMPAQ	Rouge Steel	USA(*)
BS-04	Explicit-implicit	S3BS (in-house)	300	7	Pentium III	INSA-Lyon	France
BS-05	Explicit-implicit	ABAQUS	2,304	370	SGI Origin 2000	ESTECH	Japan
BS-06	Static-implicit	Indeed 7.3.1	1,100	40	HP-UX 9000	Corus Research	The Netherlands
BS-07	Explicit-implicit	LS-DYNA3D	384	810	Sun Blade 1000	Gen. Motors	USA
BS-08	Static-implicit	ABAQUS	4,400	(?)	Pentium III	HKS, Inc.	USA
BS-09	Explicit-implicit	PAM-STAMP	3,600	40	Pentium III	Beij. U. A. A.	China
BS-10	Static-implicit	DD3 IMP	7,380	5,460	Intel Xeon	U. Coimbra	Portugal
BS-11	Static-implicit	Sheet-3	484	445	Pentium II	Ohio State U.	USA(*)
BS-12	Static-implicit	Indeed 7.3.1	4,000	480	HP-UX 9000	Corus Research	The Netherlands
BS-13	Static-implicit	ABAQUS	240	423	Pentium II	Ohio State U.	USA
BS-14	*Static-explicit*	ITAS3D	900	15	SGI Origin 2000	Inst. Phy. Chem. Res.	Japan
BS-15	Static-implicit	Indeed 7.3.1	4,000	180	HP-UX 9000	Corus Research	The Netherlands
BS-16	Explicit-implicit	PAM-STAMP	384	660	Sun Blade 1000	Gen. Motors	USA
BS-17	*Dynamic-explicit*	LS-DYNA	7,000	10	PC, 1.6 GHz	Altair Eng.	China

Fig. 4. A summary table of the computational environment data for each of the 17 simulation teams, who agreed to participate in Numisheet/NIST and contributed their results as shown in Fig. 3. *Teams BS-03 and BS-11 had no results.

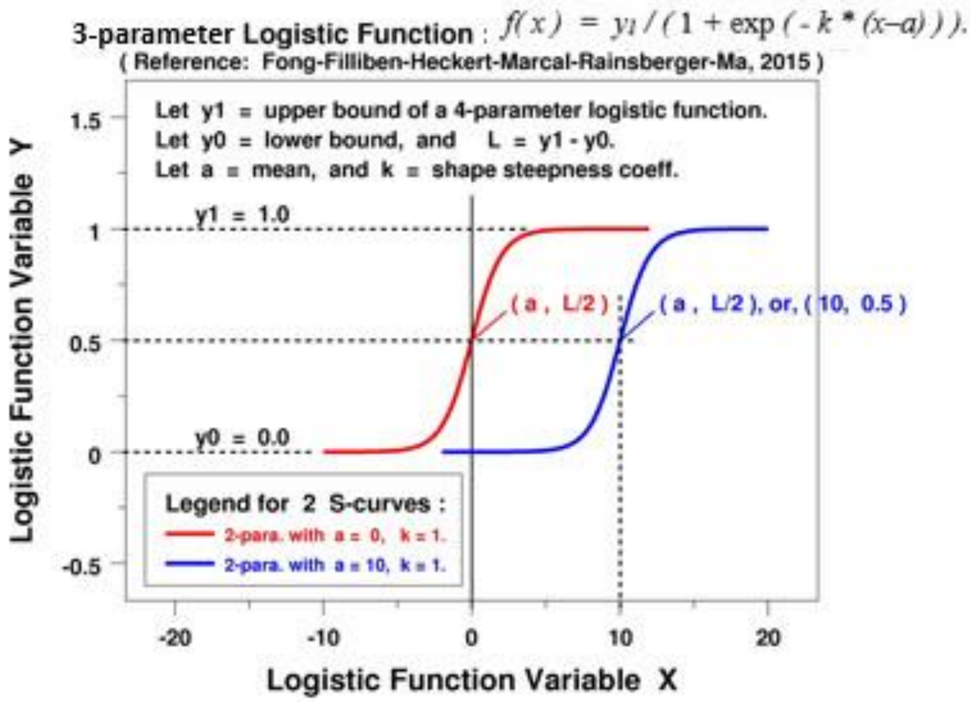

Fig. 5. A graphical plot of a 3-parameter logistic function with two values of the location parameter, a (after [17]).

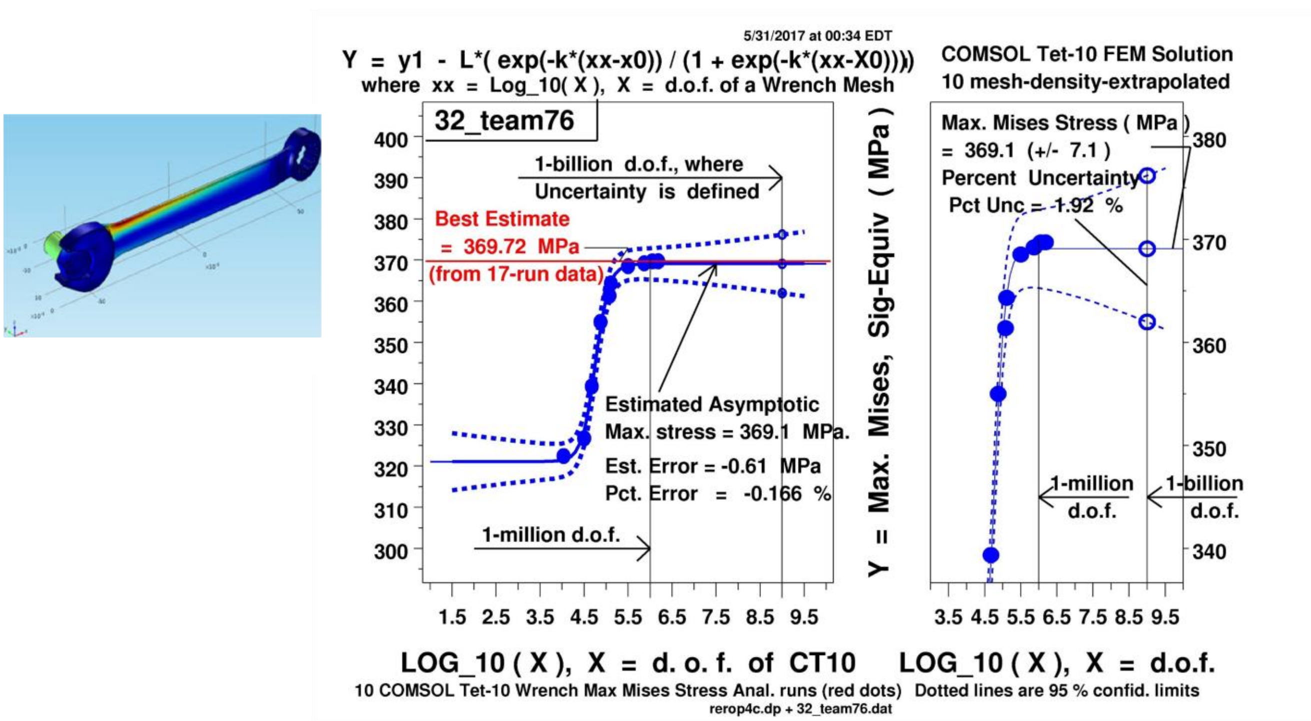

Fig. 6. A nonlinear least squares logistic Fit of 10 candidate FEA solutions for finding max. stress in a wrench [17].

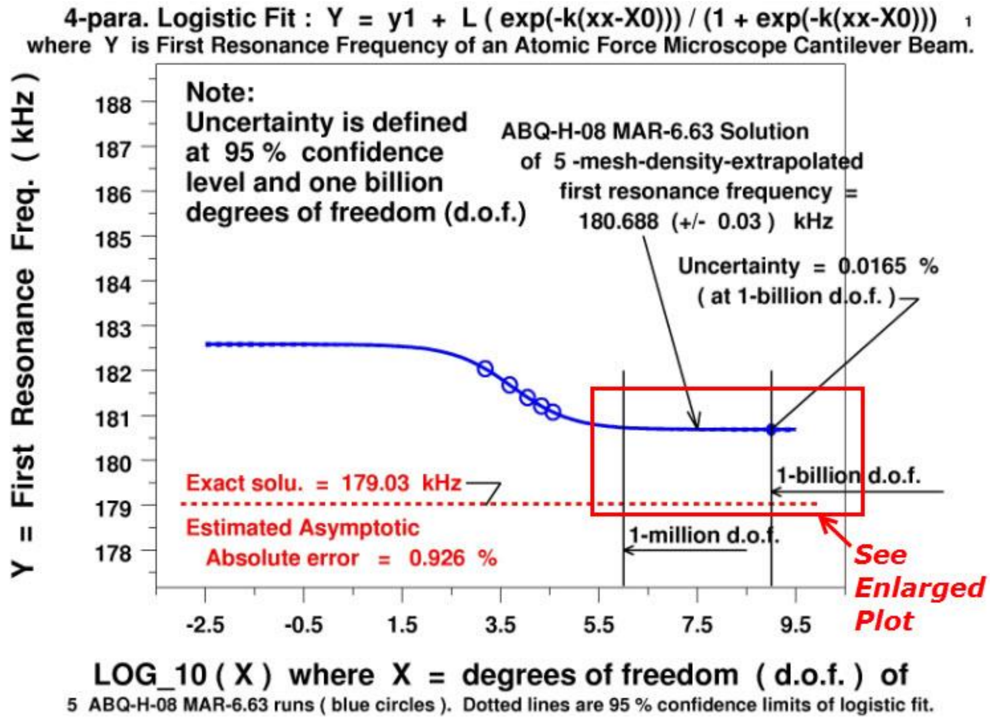

Fig. 7. A nonlinear least squares logistic fit of 5 candidate FEA solutions for finding a resonance frequency [7, 17].

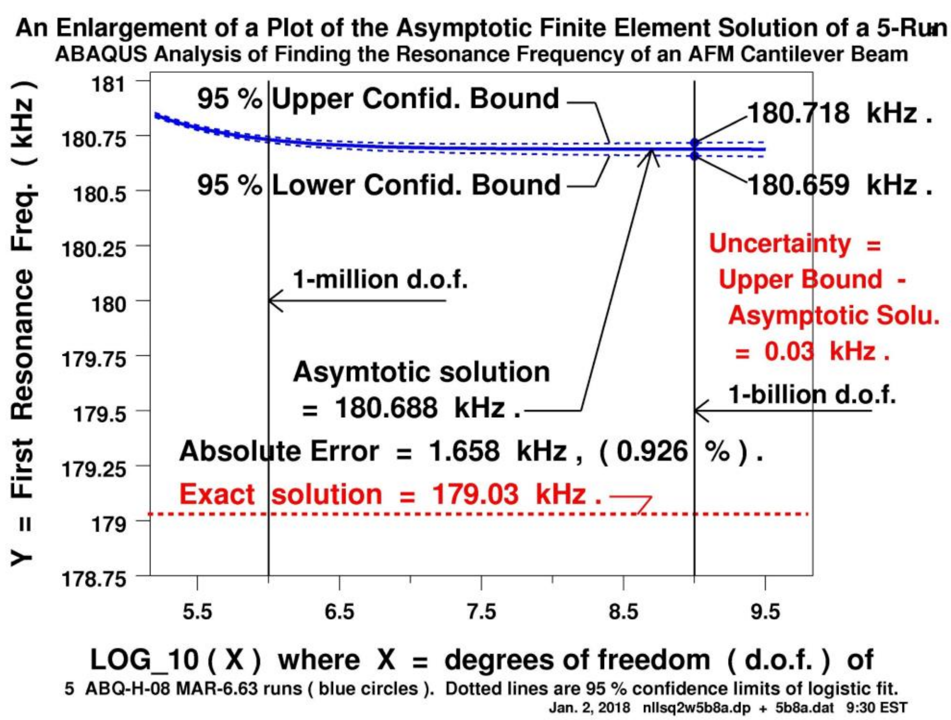

Fig. 8. An enlarged view of the asymptotic solution of a resonance frequency problem presented in Fig. 7.

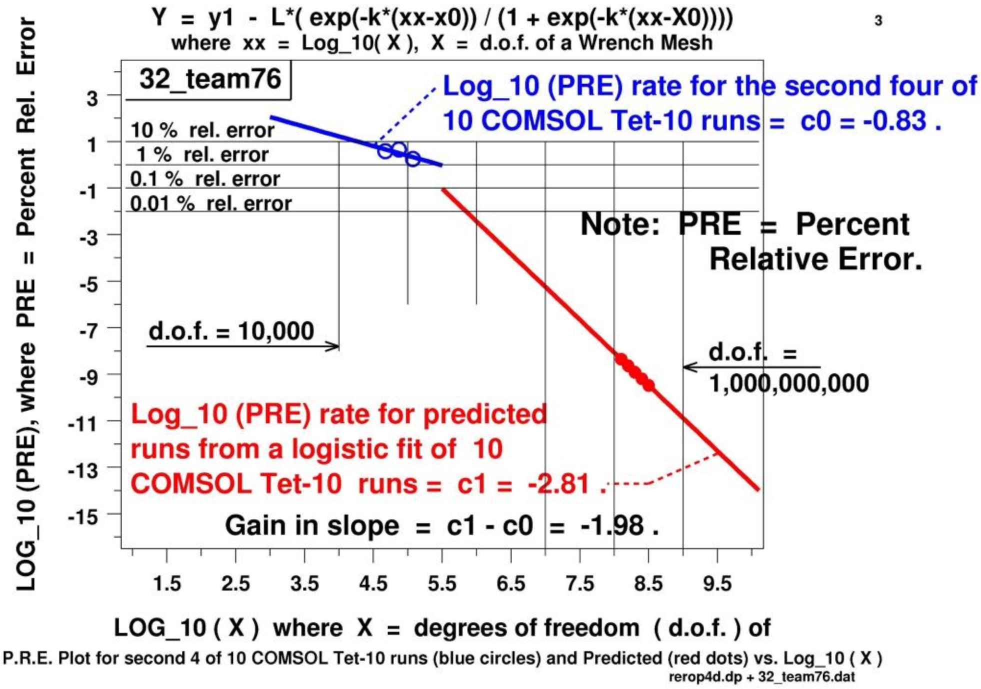

Fig. 9. Convergence behavior of 5 candidate FEA solutions before and after a nonlinear least squares fit [17].

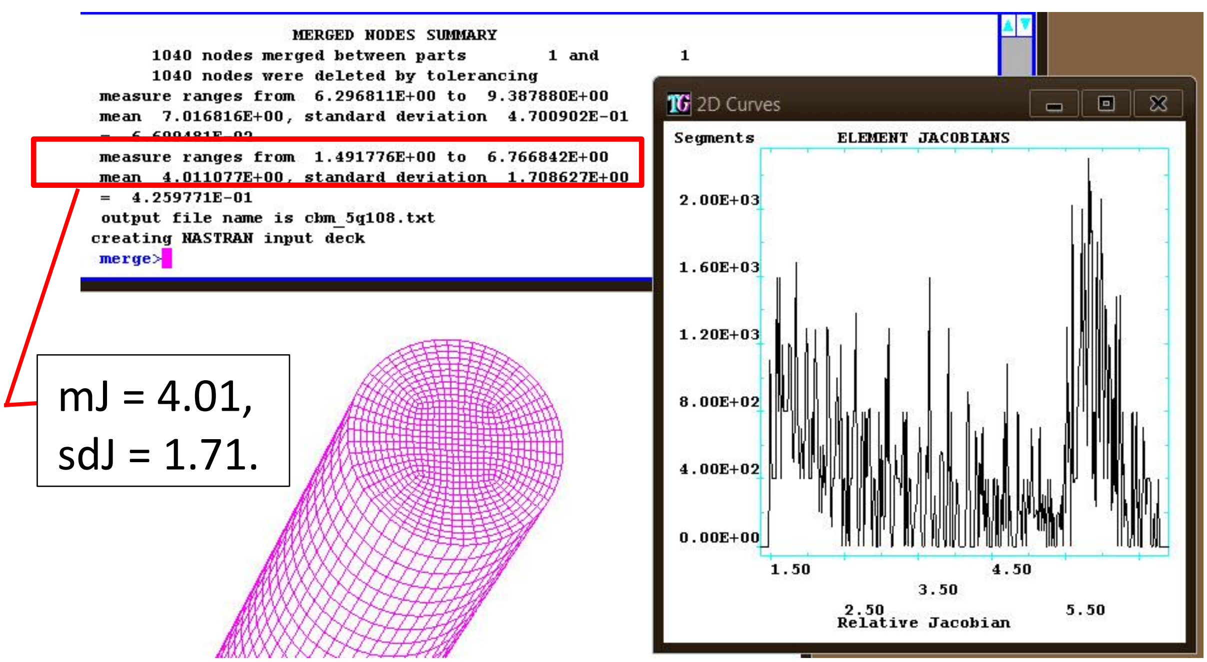

Fig. 10. An example of computing the Jacobian distribution of a finite element mesh using a *TrueGrid* macro [19, 20].

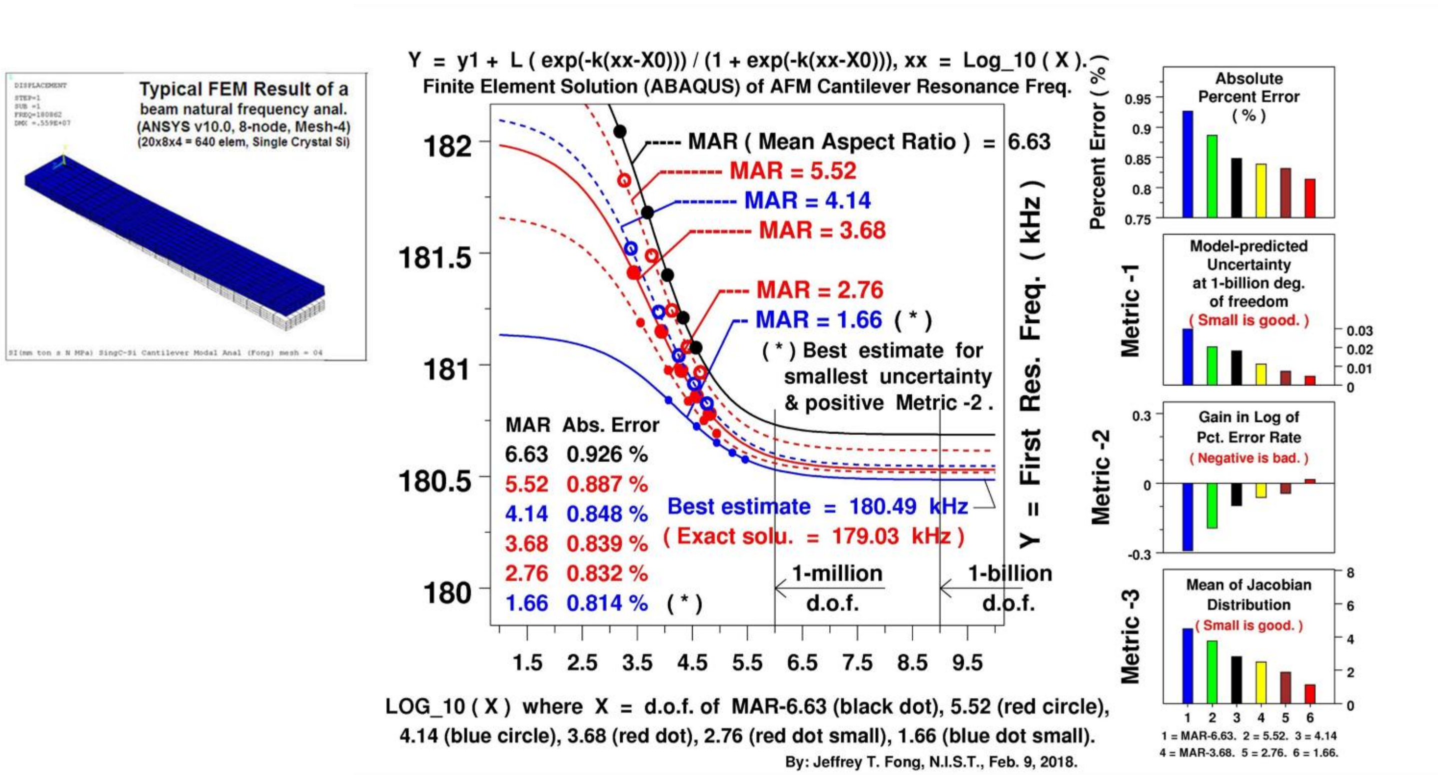

Fig. 11. Accuracy assessment of 6 FEA solutions using AAM-1, AAM-2, and AAM-3 for a resonance frequency problem.

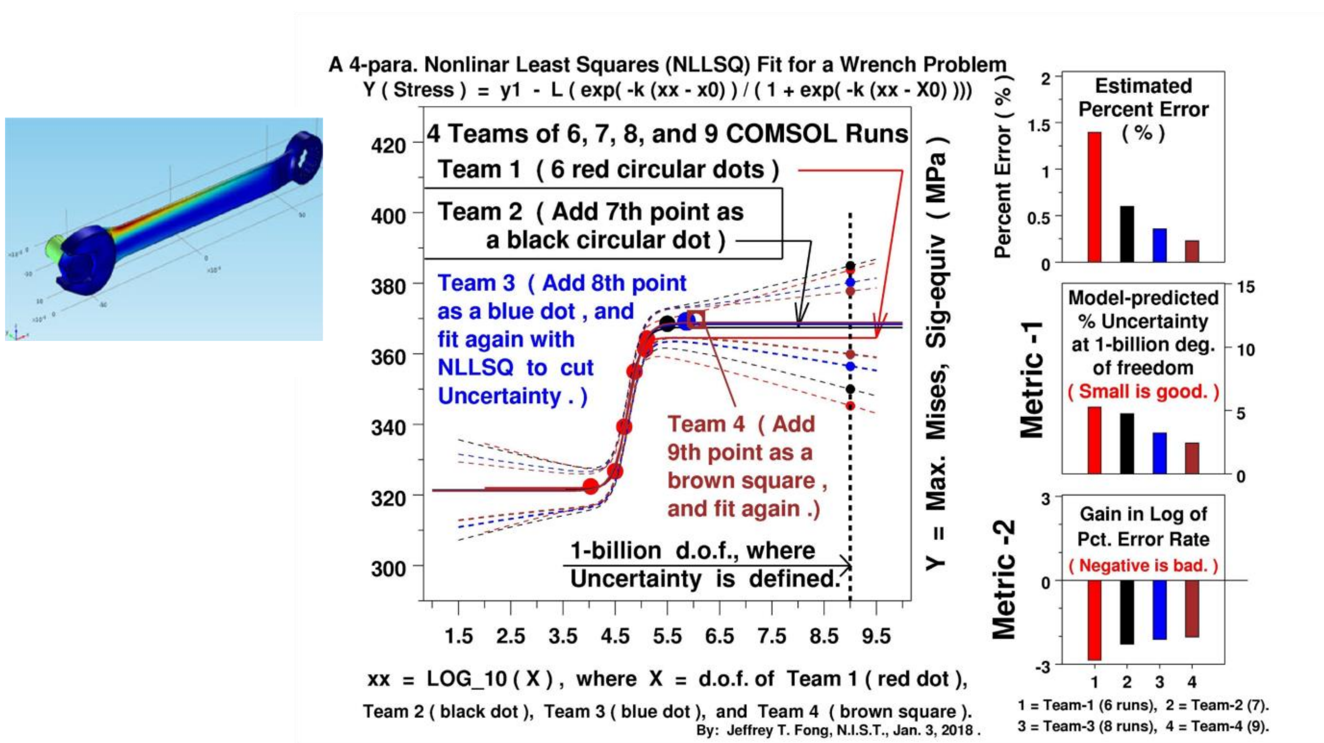

Fig. 12. Accuracy assessment of 4 FEA solutions using AAM-1 and AAM-2 for a wrench stress problem.

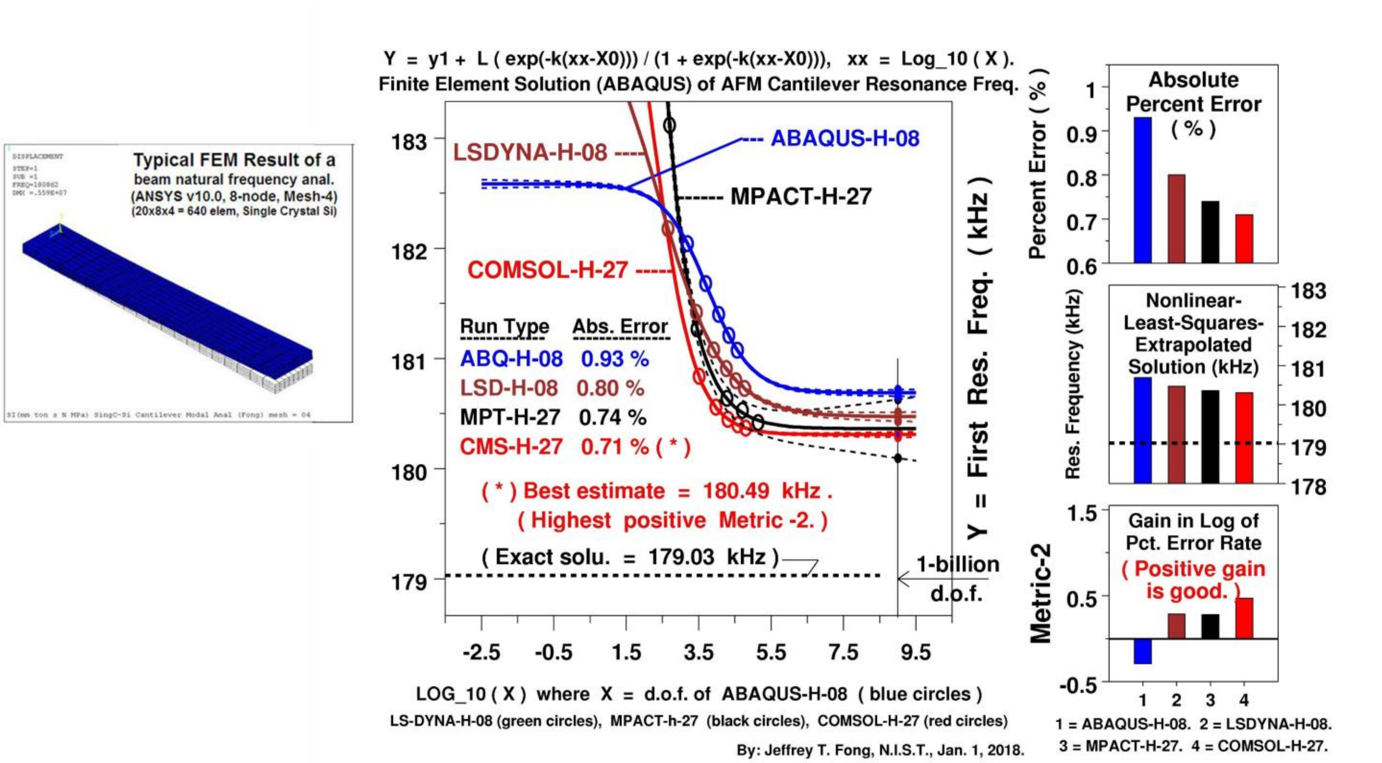

Fig. 13. Accuracy assessment of a cantilever resonance frequency solution by 4 FEA platforms using metric AAM-2.

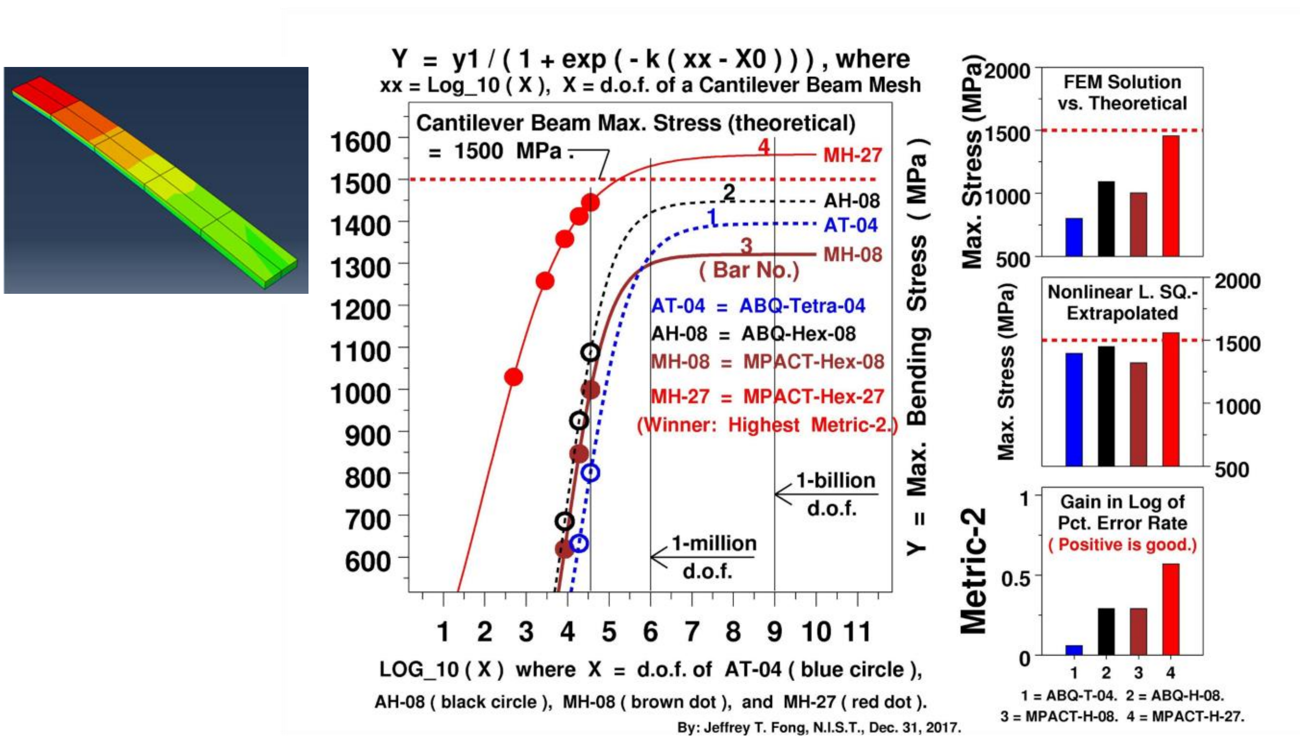

Fig. 14. Accuracy assessment of a cantilever static loading max. stress solution by 2 FEA platforms using metric AAM-2.

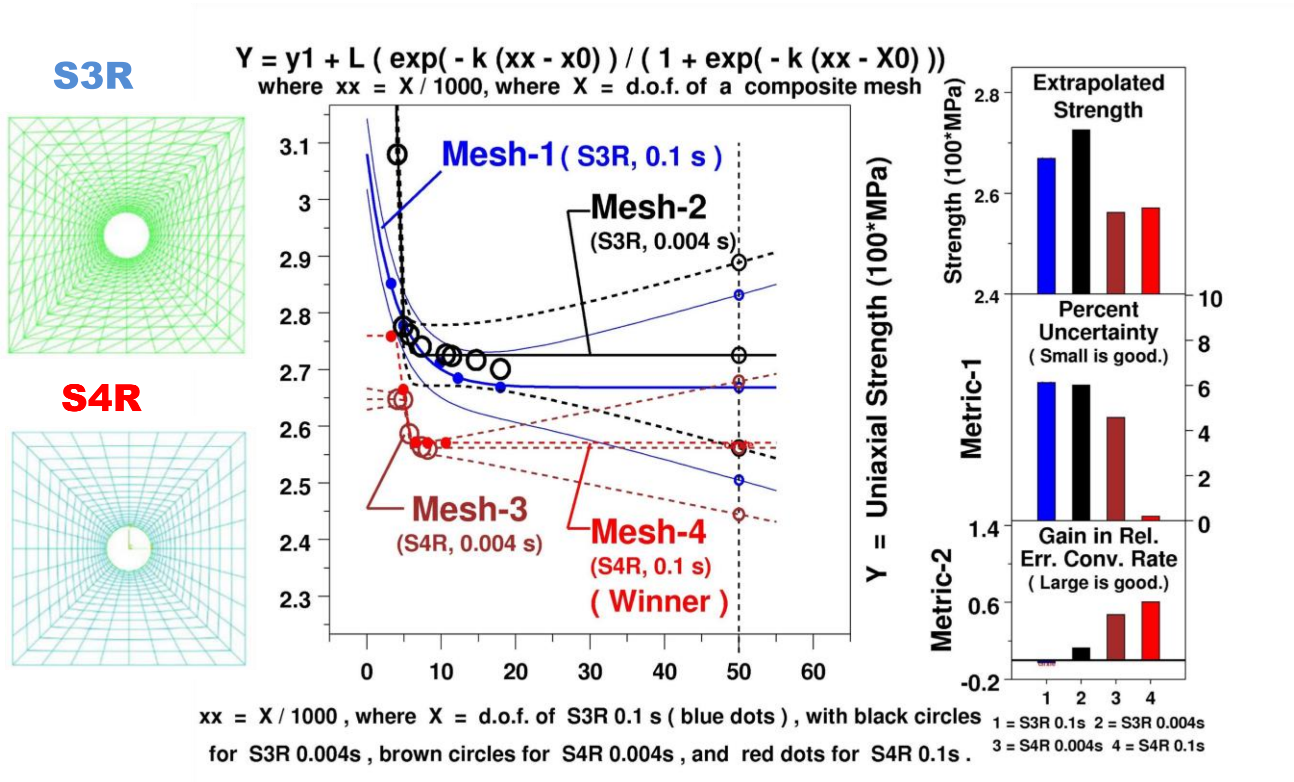

Fig. 15. Accuracy assessment of a holed composite laminate strength test with 4 FEA meshes using metrics AAM-1, -2 [21].

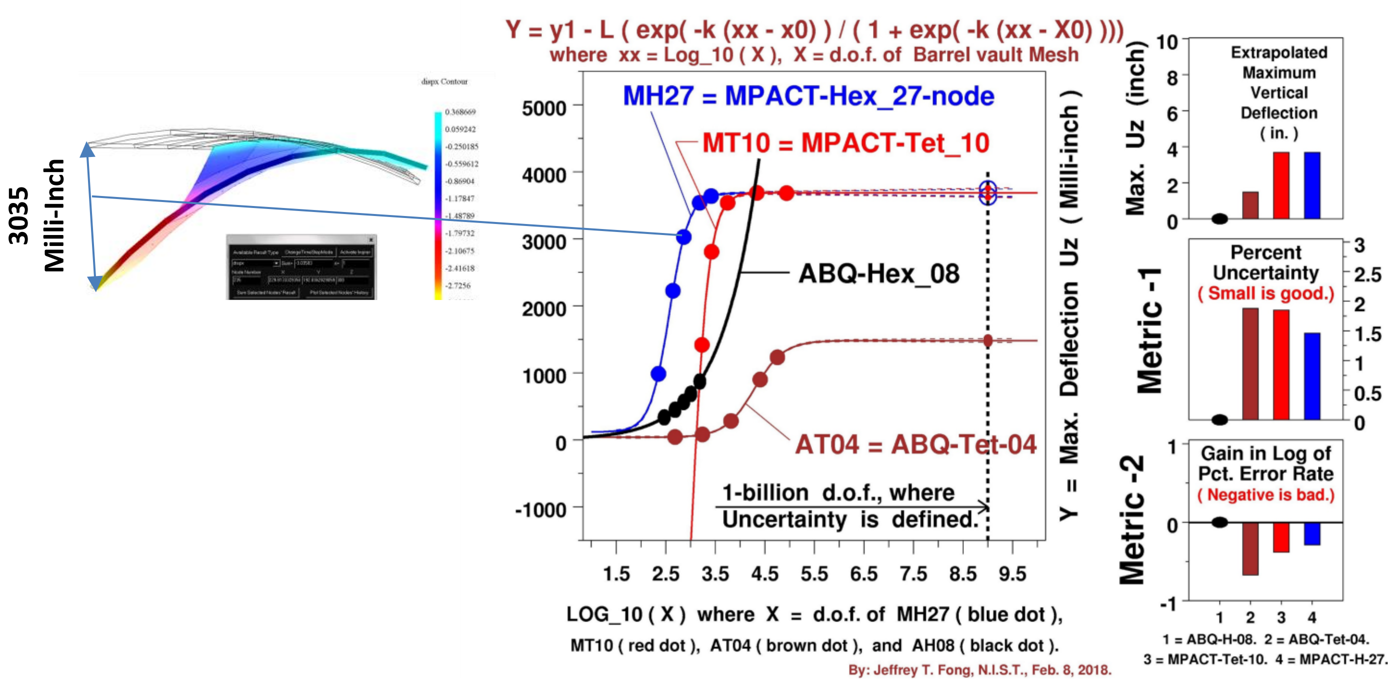

Fig. 16. Accuracy assessment of a barrel vault max. displacement solution by two FEA platforms using AAM-1 and -2.